

# Generation of amplified picosecond square pulses for low emittance electron generation in photocathode RF-GUN

Kazuya Takasago, Akira Endo  
*The Femtosecond Technology Research Association*  
5-5, Tokodai, Tsukuba, Ibaraki, 300-2635

Akira Yada, Masakazu Washio  
*Waseda University, 3-4-1, Okubo, Shinjuku-ku, Tokyo, 169-0072*

Taisuke Miura, Fumihiko Kannari  
*Department of Electrical Engineering Keio University, 3-1-1, Hiyoshi, Kohoku-ku, Yokohama, 223-8522*

Kenji Torizuka  
*National Institute of Advanced Industrial Science and Technology, 1-1-1, Umezono, Tsukuba, 305-8568*

Amplified square shaped picosecond pulses was generated for low emittance electron beam generation in a photocathode RF-GUN. Square shaped pulses were generated by using Ti:sapphire amplifier system in infrared region and then converted to ultraviolet region via third harmonics generation. Generated square shaped pulses were measured by crosscorrelation and spectral interferometric technique when the pulse duration was 1 ps, and when the pulse durations of square shaped pulses were 10 ps, these pulses were measured by streak cameras.

PACS Codes:

## Introduction

In these years, photo-cathode RF-GUN is becoming widely used to generate lower emittance electrons than using thermo-ionic emission. The photo-cathode RF-GUN can also generate shorter length electron bunches since the duration of used laser pulses in the RF-GUN is very short, such as in a picosecond or femtosecond region. Though gaussian profile picosecond pulses of frequency quadrupled Nd:YLF or Nd:YAG laser is used generally, according to recent researches it is considered that picosecond pulses with rise time in femtosecond time scale, for instance a square shaped picosecond pulse, is one of the best candidates for low emittance generation of electrons<sup>1</sup>. In order to obtain such pulses, we should utilize and place a pulse shaping apparatus, which has been developed by Weiner and co-worker at Bellcore<sup>2</sup>. In a method of pulse shaping, using the linear filtering of spatially-dispersed spectral components in a dispersion-free grating lens apparatus, the dispersed frequency components are focused onto a spatially modulated mask, such as liquid crystal spatial light modulators (LC-SLM)<sup>3</sup>, and acousto-optic modulators<sup>4</sup> at the Fourier transformed plane. The mask acts to retard and/or cut some frequency components. Finally, the pulses are transformed back into the time domain, producing a shaped waveform.

Though many demonstrations of femtosecond pulse shaping have been reported for low energy pulses directly from an oscillator, there are a few reports on amplified and shaped pulses because of low damage threshold of the modulating device. In order to obtain amplified and shaped femtosecond pulses, the pulse shaping apparatus is placed after the whole amplifier system or between the oscillator and the amplifier. When it is placed after the amplifier, it is easy to design the frequency filters since there is no distortion of modulated pulses after the pulse shaper. In this situation, however, the damage threshold of the modulation device and the insertion loss of the pulse shaper, which is about 50~90%, are serious problems. Although Brixner et al. obtained arbitrarily shaped 520  $\mu\text{J}$  femtosecond pulses from the amplified 800  $\mu\text{J}$  input pulses when the pulse shaping apparatus with a cylindrical lens pair is placed after the amplifier<sup>5</sup>, the insertion loss is still a problem in this case. On the other hand, the insertion loss of the pulse shaper can be cancelled because of saturate amplification when the pulse shaper is placed before the amplifier. Furthermore, amplified pulse of several millijoule or more than 10 mJ, which is required for the RF photocathode application, can not be applied to such pulse shaper. Hence, we have to adopt the system in which the pulse shaper is placed before the amplifier. However, when the pulse shaper is placed before the amplifier, only higher order dispersion compensation and shaping to a pulse train, not arbitrarily pulses, has been demonstrated since only phase modulation can be adopted for such a configuration to avoid damages of the optical components in the amplifier and the shaped pulses might be distorted in the amplifier.

Amplitude and phase modulation in the spectral domain can produce arbitrary pulses, although the pulse profiles are then limited by the initial spectrum, the spatial resolution of the modulation device, and the modulation area. However amplitude modulation before the pulse stretcher may cause damage to optical elements in the amplifier when pulses of several picoseconds duration are produced from femtosecond pulses, since most of the spectrum is then attenuated. For instance, consider the case of a pulse stretcher which causes a phase delay which expands 50 fs width transform-limited pulses up to 200 ps. Square shaped pulses with duration of 1 ps, generated by amplitude and phase modulation in the spectral domain will be expanded to only 10 ps and the peak intensity will be 20 times larger than in the case when the input pulse is 50 fs width transform-limited. The maximum phase modulation that can be given with a liquid crystal device is only  $10\pi$ . This is much smaller than the phase delay of the stretcher ( $\sim 200$  ps, which is  $75,000\pi$ ) and input pulses are expanded to the same width (200 ps) only if the phase of the input pulses are modulated in the spectral domain. When phase-only modulation in the spectral domain is used as the pulse shaping apparatus, we can specify only the intensity or the phase profile of output pulses in the time domain. However the intensity profile of the output pulses is the most important factor and the phase profile has no consequence in the cases of low emittance electron generation in the photocathode RF-GUN. In this paper, we demonstrate the generation of the square shaped amplified picosecond pulses with phase-only spectral modulation when the pulse shaper is placed

before the amplifier.

### Design of the phase-only spectral mask for square shaped pulses

Before describing the experiment, we shall explain how we determine the phase-only modulation on the spectral plane. According to the Fourier transform relationship, specifying the amplitude,  $A(\omega)$  and the phase,  $\phi(\omega)$  in the frequency domain specify the amplitude,  $A(t)$ , and the phase,  $\phi(t)$ , in the time domain. However when only the  $A(t)$  is specified, there exists many solutions of  $A(\omega)$  and  $\phi(\omega)$ , since  $\phi(t)$  is then a free term. In this solutions it is difficult to find a solution by analytical techniques. Therefore we use an optimisation method, developed by Kirkpatrick et al.<sup>6</sup>, which is widely used and suitable for computation. It has the ability to obtain an optimal solution without being captured at local minima because temperature exists as a waving factor in a system. Phase-only filters, designed by using the simulated annealing method, can generate arbitrary intensity shaped pulses<sup>7,8</sup>.

At first, we have confirmed that we can shape input femtosecond pulses into square shaped picosecond pulses with duration of several picoseconds with phase-only filter in a simulation. In the simulation, we used the same parameter as in the experimental case. The focal length of the lenses was 200 mm, and the number of grooves of the gratings was 1200 lines/mm for a short shaped pulse or 2400 lines/mm for a long shaped pulse, and the diffraction angle from the gratings was 21 or 73.7 degree, respectively. We used the intensity profile and the phase characteristics of the spectrum reconstructed from the experimental data of a polarization gate type frequency optical gating (PG-FROG) trace<sup>9</sup>. The central wavelength at the input pulse was ~800 nm, the spectral width was ~11 nm or ~3.5 nm and the pulse duration was ~100 fs and ~300 fs when the configuration was for short or long shaped pulse, respectively. For both cases the pulses were almost Fourier-transformed, but had slight chirps. The FROG error was sufficiently small and we also checked the reconstructed autocorrelation trace and the spectrum with one measured by the autocorrelator and the spectrometer. We assumed that the pixel width was 100  $\mu\text{m}$  and ignored the pixel gap because of the limited calculation time. Since square shaped pulses with duration of 1 to 10 ps are required for the application, 1 ps and 10 ps square shaped pulses are targeted in the simulation. The numerical result, shaped with the phase-only filter designed by the simulated annealing method, is shown in Fig. 1 when a square pulse with duration of 1 ps is targeted. The phase-only filter was designed with a phase level of 64. For 10 ps case, the result is not shown, but it is very similar to the result in the case of 1 ps. Although there remains a few pedestals before and after the main square pulse and the upper part of the pulse is a little distorted, the input 50 femtosecond quasi-sech<sup>2</sup> profile can be almost shaped into a square pulse. The size and the number of the pixels in the LC-SLM cause pedestals and distortion, so if a LC-SLM with more pixels is used we may obtain even smoother square pulses. For our applications such errors are not of major concern, since the rising time of the pulses is more important factor.

## Experimental result

In the experimental setup, we used a commercially available one-dimensional liquid-crystal spatial light modulator (Cambridge Research and Instrumentation) with 128 pixels. The period of the pixels is 100  $\mu\text{m}$  with a 3  $\mu\text{m}$  transparent gap between electrodes. A phase shift can be obtained when an electric field is applied to the electrodes, since the liquid crystal molecules tilt along the direction of thickness and cause a refractive index change for vertically polarized light. The LC-SLM can provide from 0 to  $2\pi$  shift with a resolution of  $\sim 0.01\pi$ . The input optical frequencies are spatially dispersed with a linear spatial dispersion of  $dx/d\lambda \sim 0.257$  or 1.71 mm/nm on the spectral plane, respectively. In this setup, the 52 nm or 7.5 nm spectrum was spread out on the LC-SLM. Although the throughput of this system was  $\sim 60\%$ , the power into the regenerative amplifier was strong enough for injection locking. Our amplifier consists of a home-made mode-locked Ti:sapphire laser oscillator, a Martinez-type stretcher, an all-solid-state regenerative amplifier, and a compressor. And the pulse shaper was placed between the oscillator and the stretcher.

In the experiment, we shaped the input femtosecond pulses into square shaped pulses with duration of 1 ps or 10 ps as in the numerical calculation results. The energy of the shaped pulse is about 3 mJ which is the highest energy of the arbitrarily shaped pulses to our knowledge, and we can obtain the pulse of more energy with higher pump laser in the same configuration. Although we could reconstruct the intensity profile and the phase characteristics of the unshaped pulses from the PG-FROG trace, the phase characteristics of the shaped pulses can not be reconstructed because the spectral resolution of the PG-FROG trace is not enough and applied spectral phase is too complicated to reconstruct. Hence, we measured the cross-correlation trace and spectral interference between shaped and unshaped pulses for 1 ps square shaped pulse. From measured spectral interference the spectral phase difference between the shaped and unshaped pulses can be reconstructed by easy calculation. Since spectral intensity and phase characteristics of unshaped pulse can be measured by PG-FROG method, the shaped intensity profile is reconstructed<sup>10</sup>. The experimental cross-correlation traces and intensity profile reconstructed from spectral interference are shown with the theoretical predictions in Fig. 2. Although the amplifier causes some phase distortion, the experimental results are in good agreement with numerical simulations. In the case that 10 ps duration pulse was targeted, the shaped pulse was measured directly by a streak camera with the resolution of 2 ps. The experimental intensity trace of the shaped pulse is shown in the Fig. 3. Although the rising time of the pulse is slower than the predicted one because of the time resolution, the duration and profile of the experimental result are in good agreement with the targeted one. In our case, the resolution of the shaped pulse is equal to the input pulse width of 100 fs and the shaped pulse can be generated in the range of 5.48 ps in the configuration for shorter pulse and 300 fs and 36.5 ps in the longer pulse configuration. The groove number of the gratings, the focal length of the lenses, the pixel width and the number of the pixels limit this value. In order to shape to a wider pulse width with a high temporal resolution we need to use the SLM with higher spatial resolution and more

pixels.

Furthermore, the generated square shaped infrared pulse was converted to ultraviolet region to use in the photocathode RF-GUN, since the work function of the cathode in the RF photocathode, for example, copper or magnesium, corresponds to the photon energy of the ultraviolet light. We used two BBO crystals with different thickness to generate third-order harmonics. One is type-I crystal with thickness of 3 mm for the second harmonic generation and the other is type-II crystal with thickness of 1 mm for the sum-frequency generation of the fundamental light and the second harmonic generation. With these crystals, the unshaped femtosecond infrared pulses were converted to the ultraviolet pulses with energy of about 100  $\mu\text{J}$  from 3 mJ energy. The spectral width of the converted pulse was about 0.9 nm which is wide enough to generate 10 ps square shaped pulse. When the spectral phase modulation is applied to generate shaped pulse, the output ultraviolet energy was reduced to about 20  $\mu\text{J}$  due to broadening of the pulse duration. However, that pulse can be used to generate electron in the photocathode RF-GUN. The generated square shaped ultraviolet pulse was measured by a X-ray streak camera with the resolution of 1 ps. The experimental result is shown in Fig. 4. The pulse duration is about 8 ps and rising time is a little slower than the theoretical one because of the nonlinear chirp and the spectral phase distortion in the nonlinear crystal. In order to shape to the ideal pulse shape precisely in the ultraviolet region, the precise phase characteristic of the unshaped pulse is necessary, and *in-situ* feedback system should be used to find an optimal shape automatically<sup>5</sup>.

Finally, we have also checked the beam spatial profile, which was important for our application. The beam profile of the amplified shaped pulse is shown in Fig. 5 The beam width was about 3 mm ( $1/e^2$ ) and the pattern was almost circular with a nearly gaussian beam profile. Since the beam can be focused down to 119  $\mu\text{m}$  without any speckle pattern formation with 300 mm focal length lens (the spot size of the diffraction-limited beam is 102  $\mu\text{m}$ ), its use in practical applications is not anticipated to be a problem.

### Conclusion

In conclusion, we have generated square-shaped amplified picosecond using phase-only modulation on the frequency plane for low emittance electron generation in the photocathode RF-GUN. Square shaped pulses are generated by using Ti:sapphire amplifier system in infrared region and then converted to the ultraviolet region by using the nonlinear crystals. Generated square shaped pulses were measured by crosscorrelation and spectral interferometric technique when the pulse duration was 1 ps, and when the pulse duration of the square shaped pulse was 10 ps, the shaped pulse was measured by a streak cameras. The experimental results were fairly close to the theoretically simulated pulses. Currently, we are preparing the experiment with a photocathode RF-GUN.

### Acknowledgement

The authors greatly appreciate the advice and encouragement of Dr. X. J. Wang (Brookhaven National laboratories) and Prof. Urakawa (KEK - High Energy Accelerator Research Organization). This work was performed under the management of the Femtosecond Technology Research Association (FESTA) supported by New Energy and Industrial Technology Development Organization (NEDO).

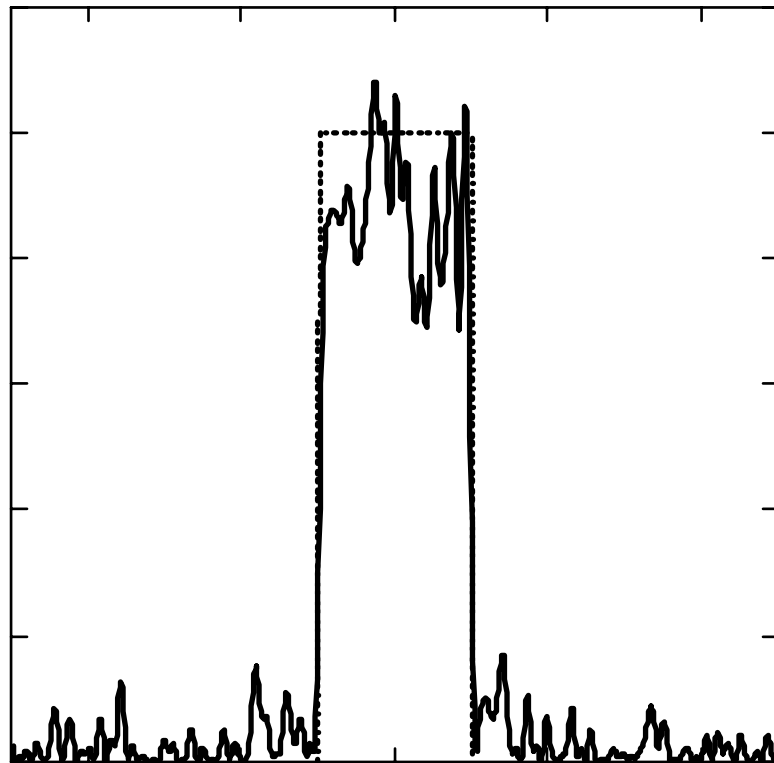
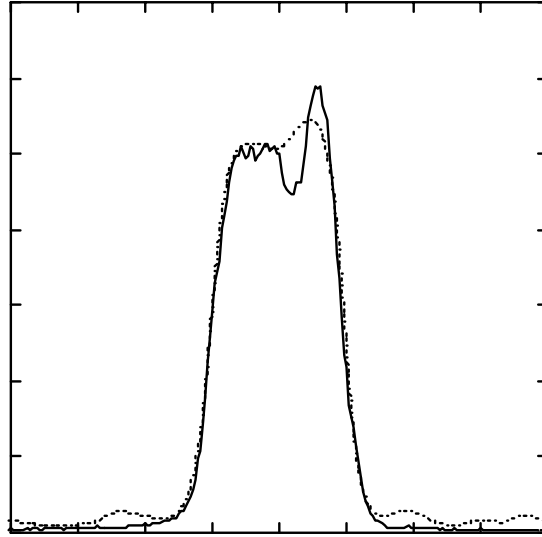


Fig. 1:

Numerical calculation result of a temporal intensity profile shaped with a 64 phase-levels mask designed by simulated annealing. The target intensity profiles are a squared shaped pulse with duration of 1 ps

(a)



(b)

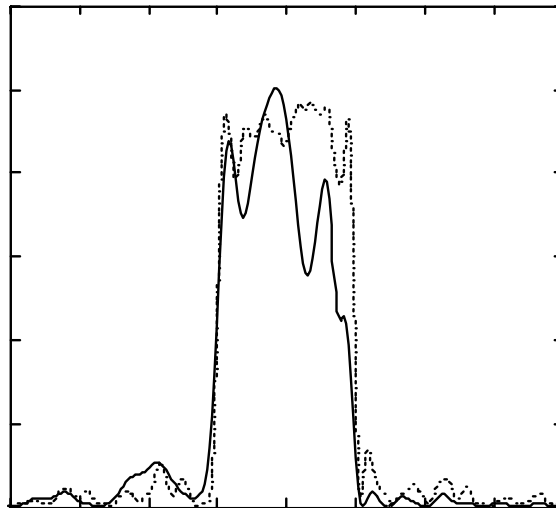


Fig. 2:

Cross-correlation measurements between the shaped pulses and the unshaped pulses (a) and temporal intensity profile of the shaped pulses calculated from the spectral intensity profile and phase characteristics reconstructed from spectral interferogram between shaped and unshaped pulses (b) with theoretical prediction (dashed curve) when a squared shaped pulse with duration of 1 ps was targeted.

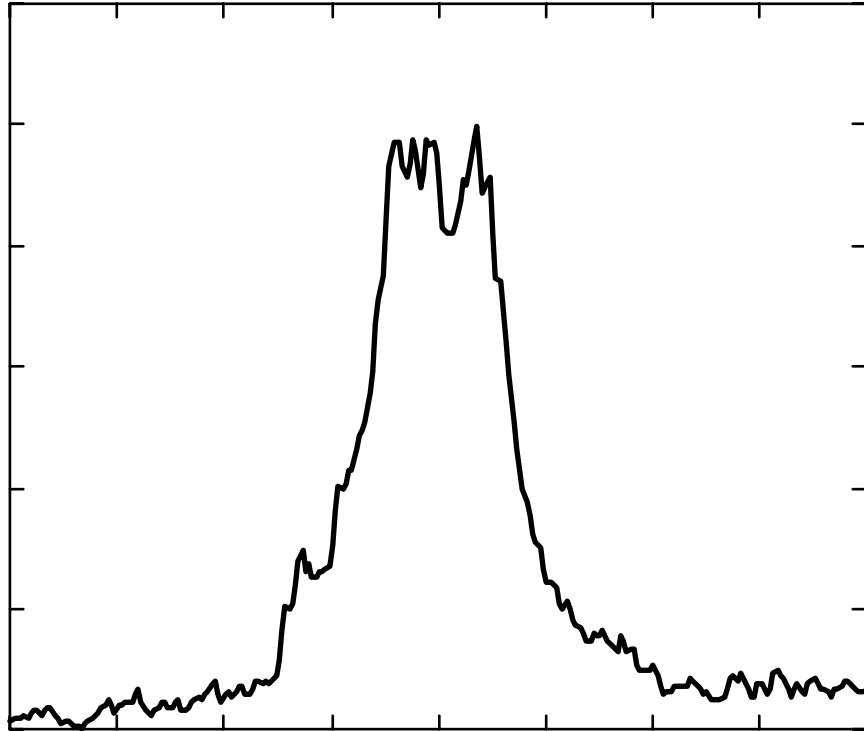


Fig. 3:

Intensity profile of the shaped pulse in infrared region measured by a streak camera when a square pulse with duration of 10 ps was targeted.

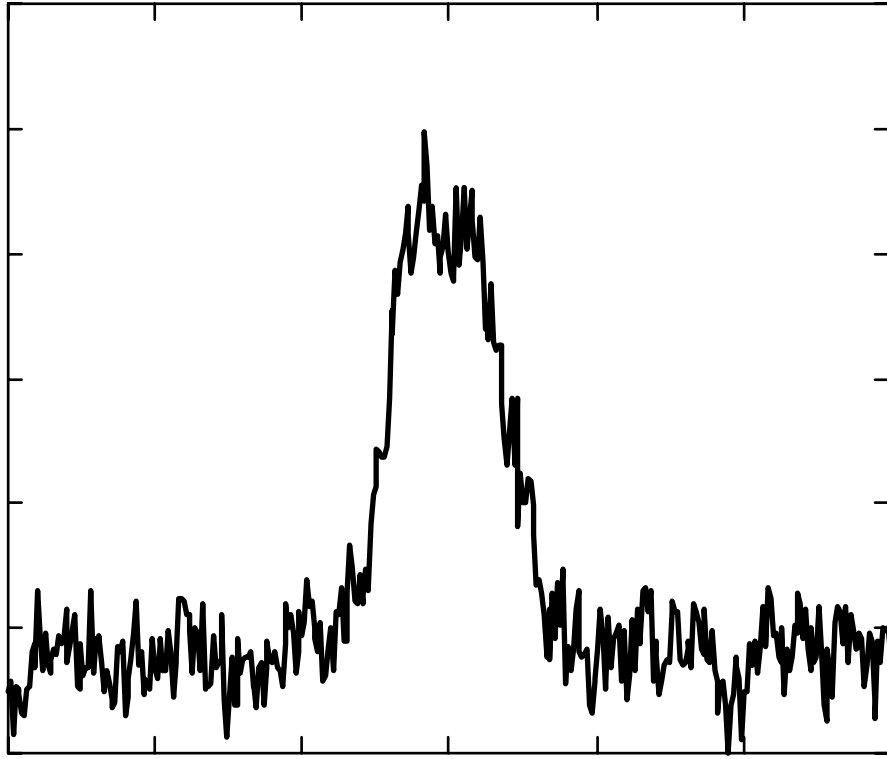


Fig.4:

Intensity profile of the shaped pulse in ultraviolet region measured by a streak camera when a square pulse with duration of 10 ps was targeted.

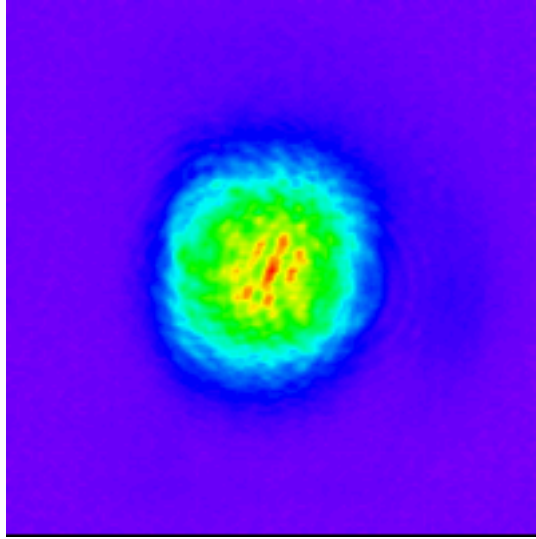


Fig.5:

Beam profile of the amplified square-shaped pulse.

- 
- <sup>1</sup> J. F. Schmerge, M. Hernandez, M. J. Hogan, D. A. Reis, and H. Winick, Proceedings of SPIE **3614**, p. 22-32 (1999).
- <sup>2</sup> A. M. Weiner, J. P. Heritage and E. M. Kirschner, J. Opt. Soc. Am. **B5**, p. 1563-1572 (1988).
- <sup>3</sup> M. M. Wefers and K. A. Nelson, Opt. Lett. **18**, p. 2032-2034 (1993).
- <sup>4</sup> M. A. Dugan, J. X. Tull and W. S. Warren, J. Opt. Soc. Am. **14**, p. 2348-2358 (1997).
- <sup>5</sup> T. Brixner, A. Oehrlein, M. Strehle and G. Gerber, Applied Physics B **70**, p. S119-S124 (2000).
- <sup>6</sup> S. Krikpatrick, C. D. Gelatt, Jr., and M. P. Vecchi, Science **220**, p. 671-680 (1983).
- <sup>7</sup> K. Takasago, M. Takekawa, F. Kannari, M. Tani and K. Sakai, Jpn. J. Appl. Phys. **35**, p. L1430-L1433 (1996).
- <sup>8</sup> K. Takasago, M. Takekawa, K. Komori and F. Kannari, IEEE J. Selected Topics in Quantum Electron. **4**, p. 346-352 (1998).
- <sup>9</sup> R. Trebino and D. J. Kane, J. Opt. Soc. Am. A **10**, p. 1101-1111 (1993).
- <sup>10</sup> D. N. Figginghoff, J. L. Bowie, J. N. Sweetser, R. T. Jennings, M. A. Krumbugel, K. W. DeLong and R. Trebino, Opt. Lett. **21**, p. 884-886 (1996).